NANO LETTERS

pubs.acs.org/NanoLett Letter

Oral Metal–Organic Gel Protected Whole-Cell Biosensor for in Situ Monitoring Nitrosamines in the Gastrointestinal Tract

Huai-Song Wang,*,+ Xing-Yu Wang,+ Hao-Tian Ding,+ Xin-Yuan Hu, Jie Li, Chen Cheng, and Feng Zheng*

Cite This: https://doi.org/10.1021/acs.nanolett.2c03418 Read Online

ACCESS | Metrics & More | Article Recommendations | Supporting Information

ABSTRACT: Nitrite, a type of food additive, has been proved convertible to genotoxic nitrosamines in the gastrointestinal tract by intestinal flora. There is no appropriate method for in situ detection of nitrosamines. Herein, plasmid-introduced *Saccharomyces cerevisiae*, which can respond to nitrosamine-induced DNA damage and activate *pMAG1*-based DNA damage repair (DDR), was designed as whole-cell biosensors (WCBs) for monitoring the in situ generated nitrosamines by a reporter gene expressing enhanced green fluorescent protein (EGFP). In order to protect the validity of WCBs (*pMAG1* yeast) from the gastric acid environment, a type of metal–organic gel (MOG), coordinated by Fe^{3+} and 2,2′-thiodiacetic acid (TDA), was prepared to embed the WCBs. The MOG(Fe-TDA) is gastric acid resistant and can deliver the *pMAG1* yeast to the gut without compromising the performance of *pMAG1* yeast to detect in situ generated nitrosamines. The genotoxicity of nitrosamines converted from nitrite was successfully detected in the gastrointestinal tract of mice.

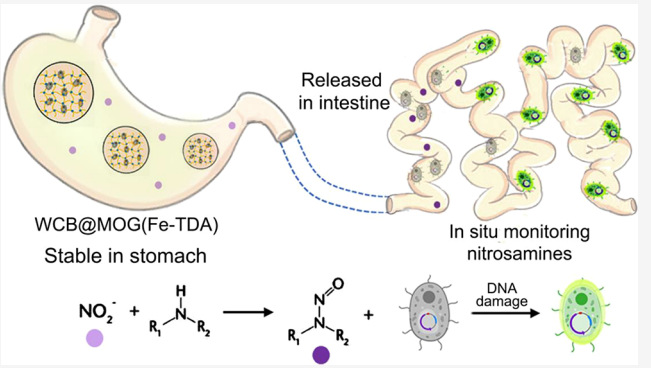

KEYWORDS: *metal–organic gel, whole-cell biosensors, nitrite, genotoxic nitrosamines, in situ detection, gastrointestinal tract*

As a type of food additive in daily life, nitrite is widely used in meat products, drinking water, vegetables, and fruits. The nitrite can be transformed to genotoxic nitrosamines by intestinal flora in the gastrointestinal tract.[1] The nitrosamines can be converted to α-hydroxynitrosamines by cytochrome P450s and then decomposed to highly active cations or diazoniums, which lead to DNA alkylation and gene mutation.[2,3] Generally, the quality control of nitrosamines in food products is detected by gas chromatography–mass spectrometry (GC–MS)[4,5] or liquid chromatography–mass spectrometry (LC-MS).[6,7] However, methods for in situ detection of nitrosamines converted from nitrite in the gastrointestinal tract are still lacking. For accurately detecting nitrosamines generated in the gastrointestinal tract, developing in situ monitoring methods is needed.

Whole-cell biosensors (WCBs), designed by plasmid introduction or gene editing in microorganisms, have the advantages of miniaturization, high throughput, simple pretreatment processes, etc.[8,9] In the WCBs, the plasmid or edited gene fragment can respond to specific analytes, and reporter protein (such as enhanced green fluorescent protein, EGFP) will be expressed.[10,11] The signal of the reporter protein can be used as an indicator. The concentration of the analytes can be detected by the signal intensity of the reporter protein.[12] Different kinds of WCBs have been widely used for detecting bioactive substances, pollutants, heavy metal ions, etc.[13,14]

Herein, we develop a type of biosensor based on WCB to detect the genotoxicity of nitrosamines converted from nitrite in the gastrointestinal tract. The WCB(yeast) is composed of the yeast *Saccharomyces cerevisiae* introduced with plasmids containing different promoters and the EGFP reporter gene. When nitrosamines cause DNA damage, the DNA damage repair (DDR) in yeast is activated, resulting in the expression of plasmids and fluorescent signal of expressed EGFP.[15] The WCB(yeast) is utilized to monitor the genotoxicity of nitrosamines converted from nitrite in gut.

However, the external environment might decrease the activity of the WCB(yeast), especially in the strong acid environment in the stomach. In order to protect WCB(yeast) from the gastric acid and deliver the WCB(yeast) to the gut, a type of metal–organic gel (MOG) was designed, which was formed by the coordination of Fe^{3+} and 2,2′-thiodiacetic acid

Received: August 29, 2022
Revised: October 15, 2022

https://doi.org/10.1021/acs.nanolett.2c03418
Nano Lett. XXXX, XXX, XXX−XXX

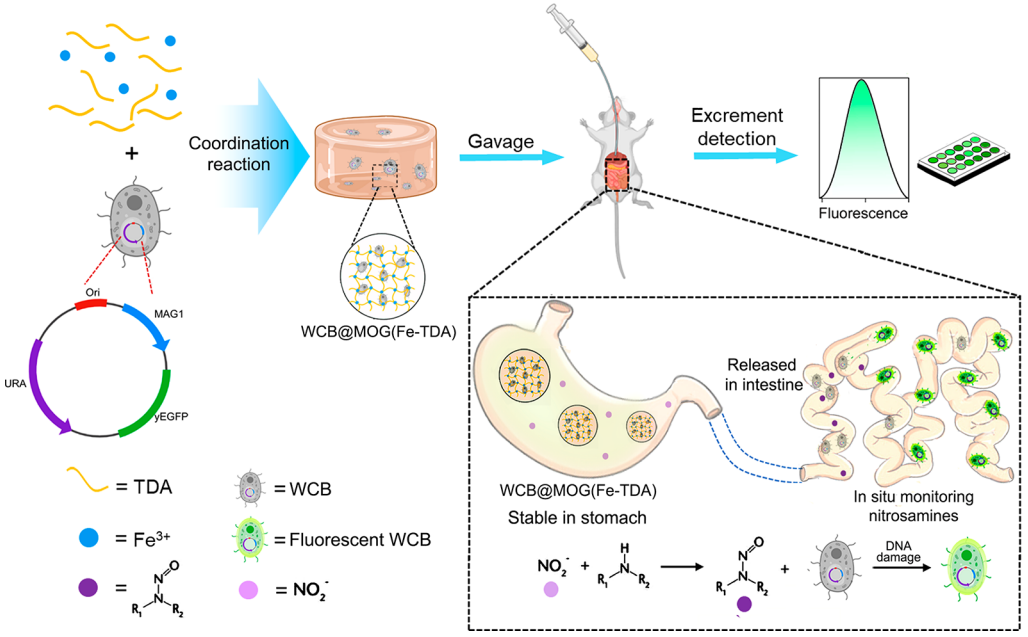

Figure 1. Schematic illustration of MOG(Fe-TDA)-encapsulated WCB(yeast) for dynamic monitoring of nitrosamine genotoxicity in the gastrointestinal tract of mice.

(TDA) at room temperature. The WCB(yeast) could be embedded in MOG(Fe-TDA) by adding the WCB(yeast) into the reaction precursor of the MOG(Fe-TDA). The MOG(Fe-TDA) was acid resistant in the stomach and could be dissolved in the gut, resulting in the release of WCB(yeast). The released WCB(yeast) was used for monitoring the nitrosamines converted from nitrite (Figure 1). The fluorescence signal of the WCB(yeast) in the feces of mouse models was detected, which could accurately detect the content of nitrosamine in the gut.

MOGs are a subclass of the hydrogel.[16,17] The hydrogel is formed by the coordination between metal ions and organic ligands, as well as other interactions, including hydrogen bonding, hydrophobic interaction, and van der Waals forces.[17−19] Noncovalent interactions enable the hydrogel to respond to mechanical, heat, electricity, and external stimuli, such as pH, temperature, pressure, light, etc. Furthermore, the morphology, size, mechanical properties, and gel formation conditions can be easily adjusted by changing the ratio and concentration of metal ions and organic ligands or reaction conditions. Therefore, MOGs have been well used in biosensing, drug release, and other fields.[20,21]

The preparation and properties of MOG(Fe-TDA) were first investigated. By adding TDA solution into Fe^{3+} solution, the MOG(Fe-TDA) could be generated under room temperature. The MOG(Fe-TDA) kept the brownish yellow color of Fe^{3+} (Figure 2A). The molecular ratio of Fe^{3+} and TDA was investigated during the preparation of MOG(Fe-TDA). It was found that when the ratio of Fe^{3+}:TDA was higher than 2:1, the gel could not be formed (Figure 2B). For the precursors with Fe^{3+}:TDA = 1:1, 2:1, and 8:1, the gel formation time was at least 5 min, 20 min, and 12 h, respectively. Therefore, the molar ratio of Fe^{3+}:TDA = 1:1 was chosen for the following experiments. The minimum precursor concentration for gel formation was 125 mM (Figure S1).

According to the transmission electron microscope (TEM) image, the morphology of the MOG(Fe-TDA) is fibrous and the width is 31.51 ± 1.77 nm (Figure 2C and Figure S2). In rheology experiments, the value of the storage modulus G' proves MOG(Fe-TDA) is formatted by coordination, because the value of the chemically covalent bond cross-linked gel usually exceeds 10^3 Pa (Figure 2D). Figure 2E−G proves the stability and injectability of MOG(Fe-TDA), which demonstrates that MOG maintains stable viscoelasticity and mechanical strength after gel−solution transition, providing data support for encapsulation of WCBs and injection. Furthermore, the MOGs(Fe-TDA) prepared with molar ratios of Fe^{3+}:TDA = 1:2 and 1:4 have been investigated (Figure S3A,B). The results show that the values of G' and G'' of MOG(Fe-TDA) (Fe^{3+}:TDA = 1:4) decrease obviously compared with that of other MOGs(Fe-TDA), indicating that the viscoelastic properties of the MOGs(Fe-TDA) (Fe^{3+}:TDA = 1:1 and 1:2) are better than that of MOG(Fe-TDA) (Fe^{3+}:TDA = 1:4) (Figure S3C).

To explore the formation mechanism of the MOGs(Fe-TDA), different ligands and metal ions were investigated. As shown in Figure S4, the ligands (diglycolic acid, thiodisuccinic acid, dimethyl 2,2′-thiobisacetate, 6,6′-dithiodinicotinic acid, 2,2′-dithiosalicylic acid) possessing groups similar to TDA were investigated to coordinate with Fe^{3+}, and TDA was used to coordinate with different metal ions. The results showed that the MOG could be generated only when TDA coordinated with Fe^{3+}. It indicated that thioether and carboxyl groups of TDA, as well as weak steric resistance, were essential for gel formation. The successful coordination between TDA and Fe^{3+} was proven by Fourier transform infrared (FT-IR) spectroscopy and ultraviolet visible (UV−vis) spectroscopy (Figure 2H and Figure S5). In the FT-IR spectrum of MOG(Fe-TDA), the $\nu_{C=O}$ signals of TDA were shifted from 1702 to 1721 cm^{-1} and the ν_{O-H} signals were shifted from 3079 to 3390 cm^{-1}, showing that the carboxyl groups of TDA were coordinated with Fe^{3+} and H_2O existed in MOG(Fe-TDA). In addition, in the UV−vis spectra, the decreased signal of the carboxyl group of TDA at 236 nm and the appearance of the absorption peak of Fe^{3+} around 360 nm proved the coordination between TDA and Fe^{3+}.

https://doi.org/10.1021/acs.nanolett.2c03418
Nano Lett. XXXX, XXX, XXX−XXX

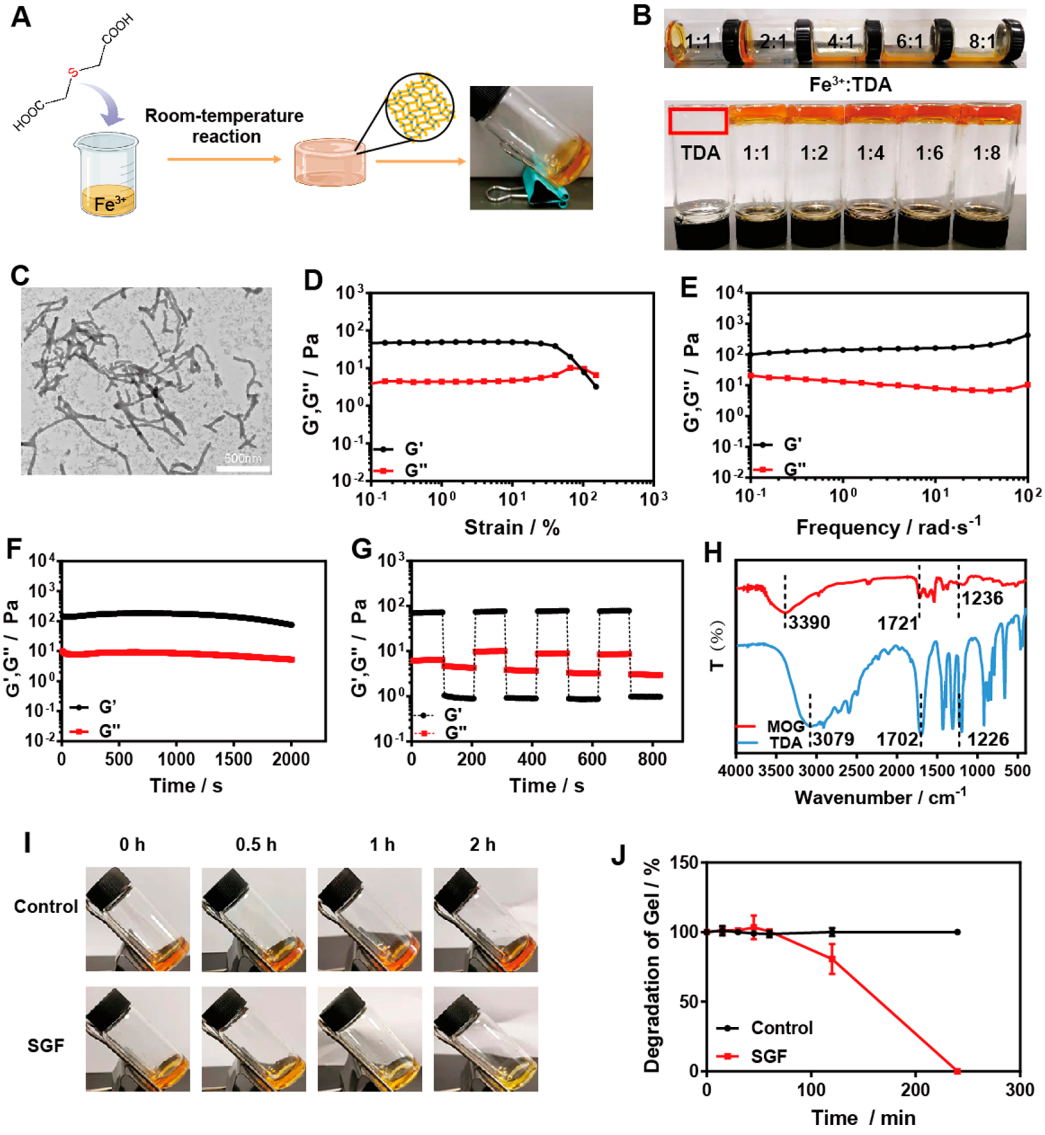

Figure 2. Preparation and characterization of MOG(Fe-TDA). (A) Schematic illustration of gel formation of MOG(Fe-TDA) at room temperature. (B) MOG(Fe-TDA) preparation with different molecular ratios of Fe^{3+} and TDA. (C) TEM image of MOG(Fe-TDA). Scale bar: 500 nm. (D) Shear moduli of MOG(Fe-TDA) with concentration 0.05 M and temperature 25 °C. (E) Rheological data of MOG(Fe-TDA) with frequency with 1% stress, 25 °C. (F) Rheological data of MOG(Fe-TDA) with high stress (130%) and low stress (1%). (G) Stability experiment of MOG(Fe-TDA) at 1% strain, 25 °C. (H) FT-IR of MOG(Fe-TDA) and TDA. (I and J) Stability of MOG(Fe-TDA) in SGF (I) and quantitative data (J) (n = 3).

Considering the MOG(Fe-TDA) being used to embed the WCB(yeast) and delivering the WCB(yeast) to the gastrointestinal tract, the stability of the MOG(Fe-TDA) in solutions with different values of pH was investigated. In vitro experiments about the degradation of the MOG(Fe-TDA) in gastric acid showed that the MOG(Fe-TDA) did not degrade until 70 min. The MOG(Fe-TDA) was degraded by 20% at 2 h, and completely degraded at 4 h (Figure 2I,J), while the MOG(Fe-TDA) kept stable in solutions with pH values of 5−8 (Figure S6). Generally, the digestion time of liquid food, or gastric emptying, was about 2 h.[22] The results showed that the degradation of MOG(Fe-TDA) was a catastrophic process around 2 h. The MOG(Fe-TDA) could remain stable in the stomach and be used to protect WCB(yeast) from degradation in simulated grastic fluid (SGF).

For monitoring nitrosamines, WCB(yeast) has been designed on the basis of DDR. DDR mainly contains the following ways: nucleotide excision repair (NER), base excision repair (BER), mismatch repair, (MMR), double-strand break repair (DSBR), translesion synthesis (TLS), direct reversal repair (DRR), DNA damage signaling (DDS), homologous recombination (HR), and nonhomologous end joining (NHEJ). DNA damage can mediate different DDR processes depending on the type of DNA damage followed by the up-regulation of a series of related proteins. In this work, WCBs(yeast) with different promoters that can up-regulate four types of proteins (*MAG1*, *PHR1*, *RAD30*, and *YKU70* respectively) during the DDR were designed. Furthermore, two yeast strains (named *pMAG1* yeast and *pPHR1* yeast), which are *pdr5* and *snq2* gene knockouts and up-regulated *MAG1* and *PHR1*, have also been investigated (Figure 3A). Information about related *S. cerevisiae* strains is listed in Table S1, and related functions of the proteins are listed in Table S2. *pdr5* and *snq2* are efflux transporters. It has been shown that

https://doi.org/10.1021/acs.nanolett.2c03418
Nano Lett. XXXX, XXX, XXX−XXX

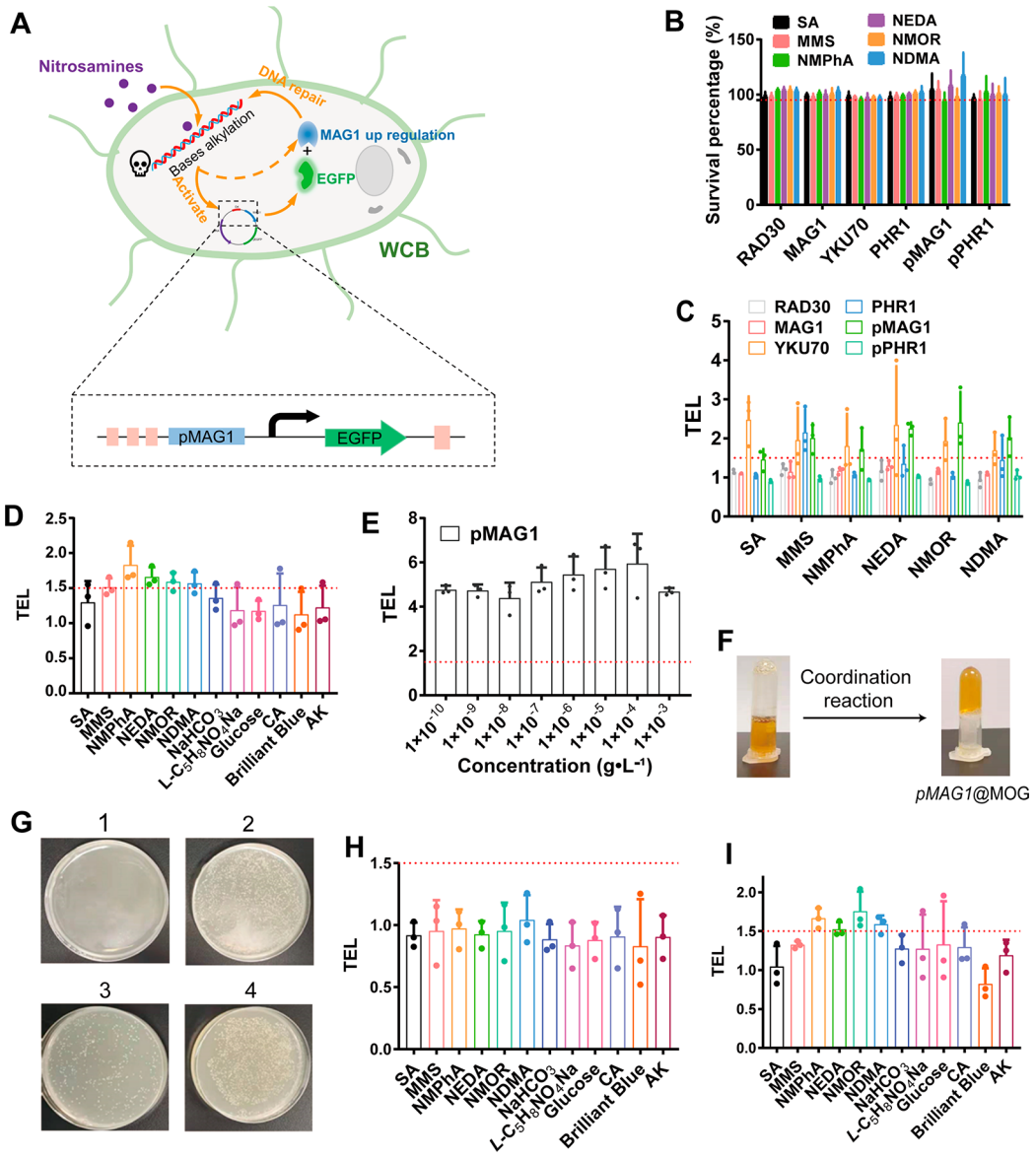

Figure 3. WCBs(yeast) for nitrosamine monitoring. (A) Schematic illustration of nitrosamines-induced DDR in WCBs(yeast) followed with the generation of fluorescent signals. (B) Survival rate of yeasts with nitrosamine. All compound concentrations are 1×10^{-3} g·L^{-1}. WCBs(yeast) were incubated at 30 °C for 24 h. (C) Responsiveness of WCBs(yeast) with different promoters to nitrosamines. The concentration of all compounds was 1×10^{-3} g·L^{-1}, and the incubation time was 30 min at 30 °C. The fluorescence signal was detected by a microplate reader. λ_{ex} = 485 nm, λ_{em} = 535 nm. (D) Specificity of *pMAG1* yeast toward nitrosamines. (E) *pMAG1* yeast for detecting NMOR with different concentrations. (F) Preparation of *pMAG1*@MOG. (G) Viability of *pMAG1*@MOG under SGF. Group 1: SGF + MOG(Fe-TDA) for 2 h. Group 2: SGF + *pMAG1* for 1 h. Group 3: SGF + *pMAG1* yeast for 2 h. Group 4: SGF + *pMAG1*@MOG for 2 h. *pMAG1*@MOG was then transferred to culture medium for 72 h, 30 °C with nitrosamine monitoring abilities of *pMAG1* yeast from Group 3 (H) and Group 4 (I) (n = 3).

the sensitivity of WCBs, which are *snq2* and *pdr5* gene knockouts, can be improved.[23] *EGFP* has been chosen as a reporter protein and inserted in the plasmid.

The nitrosamine monitoring ability of the WCBs(yeast), including *MAG1* yeast, *PHR1* yeast, *RAD30* yeast, *YKU70* yeast, *pMAG1* yeast and *pPHR1* yeast, has been investigated by choosing different compounds, including salicylic acid (SA), methylmethanesulfonate (MMS), and four nitrosamines: *N*-nitrosodimethylamine (NDMA), *N*-nitrosodiethylamine (NDEA), *N*-nitrosomethylaniline (NMPhA), and *N*-nitrosomorpholine (NMOR). Among them, SA is the negative control without responsiveness, while MMS is the positive control. The yeasts in the logarithmic growth phase have been selected (Figure S7). Figure 3B shows that when the concentration of the compounds is 1×10^{-3} g·L^{-1}, all of the survival rates of the WCBs(yeast) are over 95%. Therefore, the concentrations of all compounds are not higher than 1×10^{-3} g·L^{-1} during investigating the nitrosamine monitoring abilities of the WCBs(yeast). Then, the pathway of nitrosamine-induced DNA damage is explored in Figure 3C. A TEL (total protein expression level) value of 1.5 is used as the limit of detection. When the TEL value exceeds 1.5, the tested compound can be considered to be genotoxic.[24−26] Figure 3C shows that only *pMAG1* yeast and *YKU70* yeast respond to the nitrosamines, while *YKU70* yeast also responds to negative control SA. This indicates that nitrosamine-mediated DDR is through the BER pathway for DNA damage repair (Figure

https://doi.org/10.1021/acs.nanolett.2c03418
Nano Lett. XXXX, XXX, XXX−XXX

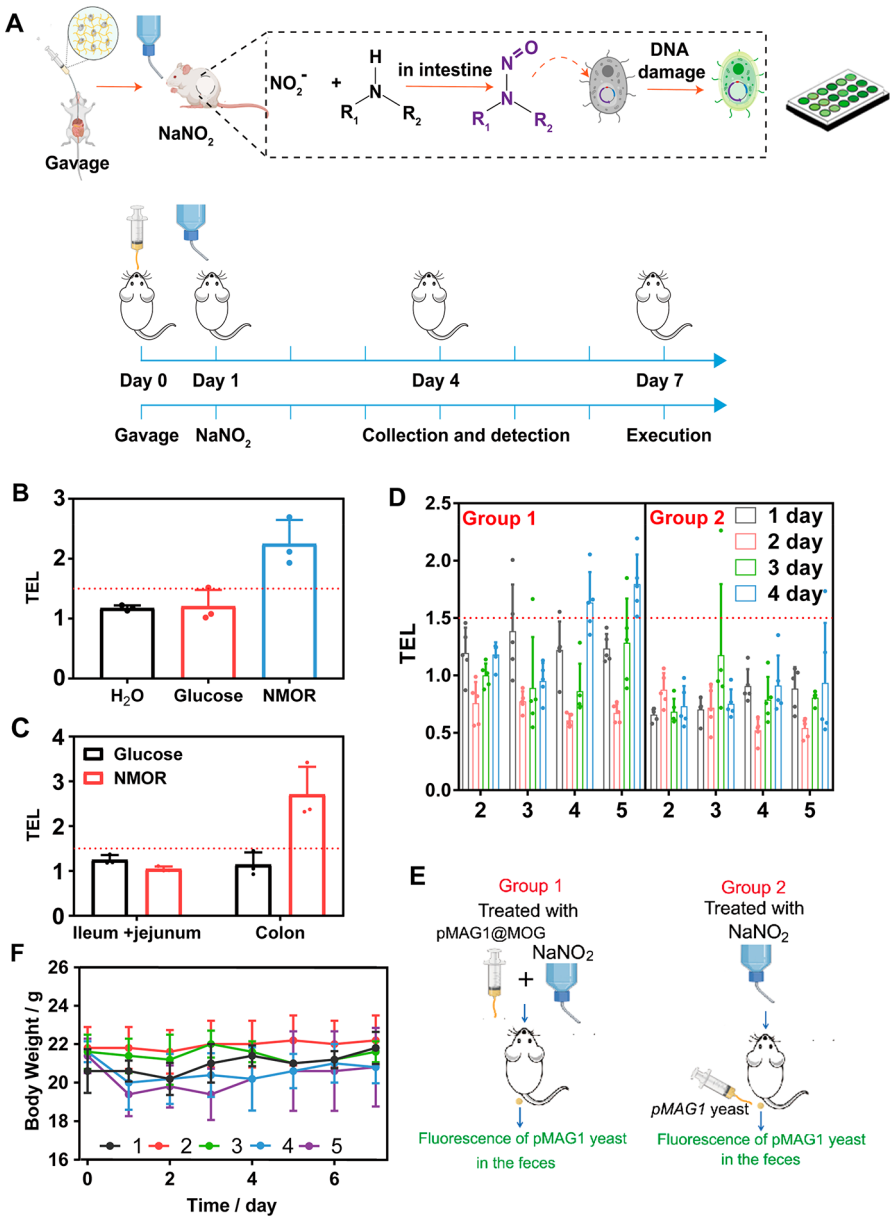

Figure 4. In vivo nitrosamine monitoring by *pMAG1*@MOG. (A) Flowchart and timetable of gavage experiment. (B) Detection of NMOR in drinking water. The concentration of glucose or NMOR was 0.68 mg·L^{-1}. (C) Detection of fluorescent signal of *pMGA1* yeast in different intestinal sites. (D–F) Detection of fluorescent signal of *pMAG1* yeast in feces at different days (D), illustration of the mice grouping (E), and body weight of mice with different groups (F). The TEL value represents the genotoxicity of nitrite conversion to nitrosamines. Data points represent the mean ± SD (n = 5). Group 1: MOG(Fe-TDA). Group 2: MOG(Fe-TDA) + $NaNO_2$ (50 mg/kg/day). Group 3: *pMAG1* yeast + $NaNO_2$ (50 mg/kg/day). Group 4: *pMAG1*@MOG + $NaNO_2$ (50 mg/kg/day). Group 5: *pMAG1*@MOG + $NaNO_2$ (5 mg/kg/day). Data points represent the mean ± SD (n = 5).

3A). Therefore, the *pMAG1* yeast and NMOR with the highest TEL values have been selected for the following experiments.

To investigate the specificity of the *pMAG1* yeast for monitoring nitrosamines, several compounds commonly used in food additives, such as $NaHCO_3$, acesulfame K (AK), glucose, L-$C_5H_8NO_4Na$, citric acid (CA), and brilliant blue, were tested Figure 3D. The results showed that *pMAG1* yeast could especially respond to nitrosamines with concentrations as low as 1 × 10^{-10} g·L^{-1} (Figure 3E). Then, MOG(Fe-TDA) embedded with *pMAG1* yeast (*pMAG1*@MOG) was successfully prepared by adding *pMAG1* yeast into the precursor of MOG(Fe-TDA) (Figure 3F). The protective effect of MOG(Fe-TDA) for *pMAG1* yeast in the gastric acid was investigated. After being exposed to gastric acid for 1 or 2 h, the *pMAG1* yeast in the *pMAG1*@MOG showed higher colony numbers in the medium compared with *pMAG1* yeast directly exposed to gastric acid (Figure 3G). According to the nitrosamine monitoring results, *pMAG1* yeast directly exposed to gastric acid showed no response to nitrosamines (Figure 3H), while the *pMAG1* yeast in *pMAG1*@MOG maintained the performance of nitrosamine response ability after being exposed to gastric acid (Figure 3I).

The survival rate of *pMAG1* yeast after being embedded in *pMAG1*@MOG for different times was further investigated. Figure S8 showed that when *pMAG1* yeast was encapsulated in MOG(Fe-TDA) for 2 h, *pMAG1* yeast could survive and

https://doi.org/10.1021/acs.nanolett.2c03418
Nano Lett. XXXX, XXX, XXX−XXX

colonies could be observed in the culture medium. In addition, if the *pMAG1*@MOG was immersed in SGF within 2 h, the survived *pMAG1* yeast could also be observed, showing the protection ability of the MOG(Fe-TDA) for *pMAG1* yeast. However, after being encapsulated in MOG(Fe-TDA) for 4 h, there were few *pMAG1* yeasts observed in the culture medium, even incubated for 96 h. In this work, the *pMAG1* yeast would be released from the *pMAG1*@MOG within 2 h. Therefore, the *pMAG1*@MOG could be used for delivering the *pMAG1* yeast into the gastrointestinal tract to monitor the in situ generated nitrosamines.

In order to verify the in situ nitrosamine monitoring ability of *pMAG1*@MOG, an animal experiment was performed. Nitrates were used as the model, which could be transformed to nitrosamines by intestinal flora and would be absorbed and accumulated in the body.[27] By detecting the fluorescence intensity of *pMAG1* yeast in the feces of animals, the in situ generated nitrosamines could be observed (Figure 4A). The NMOR and glucose in drinking water were first detected by in vitro experiments, showing that the *pMAG1*@MOG could reflect the genotoxicity of nitrosamines (Figure 4B). The value of TEL of NMOR was 2.25, indicating that *pMAG1*@MOG had a good detection effect.

Then, Balb/c mice were chosen for gavage of pMAG1@MOG and drinking water containing NMOR. The intestinal tract of the mice was dissected, and the fluorescence signal of *pMAG1* yeast was detected on the fourth day (Figure 4C). No obvious fluorescence signal was detected in the ileum and jejunum. The TEL values of both the glucose group (negative control) and the NMOR group were 1.18 and 1.05, which were not more than 1.5. This indicated that *pMAG1* yeast did not proliferate in the ileum and jejunum, while fluorescence signals were detected in the colon and the TEL value of NMOR was 2.71. It showed that the reproduction site of *pMAG1* yeast was mainly in the colon, and this method could be used to detect nitrosamines.

Furthermore, *pMAG1*@MOG was used to monitor the nitrosamines converted from nitrite. The Balb/c mice were fed with drinking water containing $NaNO_2$ and treated with *pMAG1*@MOG. The fluorescence signal of *pMAG1* yeast in the feces was detected. The detection results from day 1 to day 4 were displayed in Figure 4D. It showed that genotoxicity was detectable at day 4 for the mice treated with both high and low concentrations of $NaNO_2$. However, it was not detected in the first 3 days, which might be due to the fact that *pMAG1* yeast had not yet proliferated to a certain number in the colon, which was consistent with the result of in vitro experiments. However, fecal nitrosamines were not detected by *pMAG1* yeast in the mice group which was not treated with *pMAG1*@MOG (Figure 4E). It might be due to the uptake of nitrosamines by the gastrointestinal tract. It also showed that the developed method was more accurate for the in situ monitoring of the generation of nitrosamine than the traditional in vitro detection methods. During the detection, there was no significant change in the body weight of Balb/c mice (Figure 4F).

In summary, a type of MOG, MOG(Fe-TDA), was prepared by the coordination between Fe^{3+} and TDA. The MOG(Fe-TDA) with the molar ratio Fe^{3+}:TDA = 1:1 was stable in the gastric acid environment within 2 h. MOG(Fe-TDA) shows ideal protective ability to deliver yeast-based WCBs (*pMAG1* yeast) into the gastrointestinal tract to monitor in situ generated nitrosamines. The *pMAG1* yeast could monitor nitrosamines with concentrations as low as 1×10^{-10} g·L^{-1} via the fluorescence intensity of expressed EGFP. After being embedded in MOG(Fe-TDA), the *pMAG1* yeast could remain active for 2 h. Therefore, *pMAG1*@MOG was used to deliver the *pMAG1* yeast into intestinal tract in the animal experiment. The results showed that the *pMAG1* yeast delivered by pMAG1@MOG could be proliferated in the intestinal tract, and the genotoxicity of nitrosamines transformed from nitrite was successfully detected.

■ ASSOCIATED CONTENT

Supporting Information

The Supporting Information is available free of charge at https://pubs.acs.org/doi/10.1021/acs.nanolett.2c03418.

Chemicals and reagents, apparatus, synthesis of MOG-(Fe-TDA), stability of MOG(Fe-TDA) in gastric acid, yeast strains and culture, fluorescence measurements, pMAG1 yeast protection ability of MOG(Fe-TDA), in vivo experiments, rheological data of MOG(Fe-TDA), fiber widths, UV−vis spectra, photographs showing preparation and stability of MOG(Fe-TDA) and formation of MOG, growth curves, and survival rate of *pMAG1* yeast in *pMAG1*@MOG (PDF)

■ AUTHOR INFORMATION

Corresponding Authors

Huai-Song Wang − *Key Laboratory of Drug Quality Control and Pharmacovigilance (Ministry of Education), China Pharmaceutical University, Nanjing 210009, China; Department of Pharmaceutical Analysis, China Pharmaceutical University, Nanjing 210009, China;* orcid.org/0000-0001-7892-018X; Email: wanghuaisong@cpu.edu.cn, wanghuai1234@gmail.com

Feng Zheng − *Key Laboratory of Drug Quality Control and Pharmacovigilance (Ministry of Education), China Pharmaceutical University, Nanjing 210009, China; Department of Pharmaceutical Analysis, China Pharmaceutical University, Nanjing 210009, China;* Email: cpu_analyst@126.com

Authors

Xing-Yu Wang − *Key Laboratory of Drug Quality Control and Pharmacovigilance (Ministry of Education), China Pharmaceutical University, Nanjing 210009, China*

Hao-Tian Ding − *Key Laboratory of Drug Quality Control and Pharmacovigilance (Ministry of Education), China Pharmaceutical University, Nanjing 210009, China*

Xin-Yuan Hu − *Key Laboratory of Drug Quality Control and Pharmacovigilance (Ministry of Education), China Pharmaceutical University, Nanjing 210009, China*

Jie Li − *Key Laboratory of Drug Quality Control and Pharmacovigilance (Ministry of Education), China Pharmaceutical University, Nanjing 210009, China*

Chen Cheng − *Key Laboratory of Drug Quality Control and Pharmacovigilance (Ministry of Education), China Pharmaceutical University, Nanjing 210009, China*

Complete contact information is available at: https://pubs.acs.org/10.1021/acs.nanolett.2c03418

https://doi.org/10.1021/acs.nanolett.2c03418
Nano Lett. XXXX, XXX, XXX−XXX

Author Contributions

[+]H.-S. Wang, X.-Y. Wang and H.-T. Ding contributed equally to this work.

Notes

The authors declare no competing financial interest.

■ ACKNOWLEDGMENTS

This work was supported by the National Natural Science Foundation of China (21705165 and 82073815), the Open Project Program of MOE Key Laboratory of Drug Quality Control and Pharmaco vigilance (No. DQCP20/21MS03), and Double First-rate discipline construction (No. CPU2022QZ12).

■ REFERENCES

(1) Lundberg, J. O.; Weitzberg, E. Biology of nitrogen oxides in the gastrointestinal tract. *Gut.* **2013**, *62* (4), 616.

(2) Li, X.; He, X.; Le, Y.; Guo, X.; Bryant, M. S.; Atrakchi, A. H.; McGovern, T. J.; Davis-Bruno, K. L.; Keire, D. A.; Heflich, R. H.; Mei, N. Genotoxicity evaluation of nitrosamine impurities using human TK6 cells transduced with cytochrome P450s. *Arch. Toxicol.* **2022**, *96* (11), 3077−3089.

(3) Carlson, E. S.; Upadhyaya, P.; Hecht, S. S. Evaluation of nitrosamide formation in the cytochrome P450-mediated metabolism of tobacco-specific nitrosamines. *Chem. Res. Toxicol.* **2016**, *29* (12), 2194−2205.

(4) Akyuz, M.; Ata, S.; Dinc, E. A chemometric optimization of method for determination of nitrosamines in gastric juices by GC-MS. *J. Pharmaceut. Biomed.* **2016**, *117*, 26−36.

(5) Wichitnithad, W.; Sudtanon, O.; Srisunak, P.; Cheewatanakornkool, K.; Nantaphol, S.; Rojsitthisak, P. Development of a sensitive headspace gas chromatography-mass spectrometry method for the simultaneous determination of nitrosamines in losartan active pharmaceutical ingredients. *ACS Omega.* **2021**, *6* (16), 11048−11058.

(6) Chang, S. H.; Chang, C. C.; Wang, L. J.; Chen, W. C.; Fan, S. Y.; Zang, C. Z.; Hsu, Y. H.; Lin, M. C.; Tseng, S. H.; Wang, D. Y. A multi-analyte LC-MS/MS method for screening and quantification of nitrosamines in sartans. *J. Food Drug Anal.* **2020**, *28* (2), 98−107.

(7) Li, Z.; Wang, J.; Chen, X.; Hu, S.; Gong, T.; Xian, Q. A novel molecularly imprinted polymer-solid phase extraction method coupled with high performance liquid chromatography tandem mass spectrometry for the determination of nitrosamines in water and beverage samples. *Food Chem.* **2019**, *292*, 267−274.

(8) Moraskie, M.; Roshid, M. H. O.; O'Connor, G.; Dikici, E.; Zingg, J.-M.; Deo, S.; Daunert, S. Microbial whole-cell biosensors: Current applications, challenges, and future perspectives. *Biosens. Bioelectron.* **2021**, *191*, 113359.

(9) van der Meer, J. R.; Belkin, S. Where microbiology meets microengineering: design and applications of reporter bacteria. *Nat. Rev. Microbiol.* **2010**, *8* (7), 511−522.

(10) Lee, W.; Kim, H.; Kang, Y.; Lee, Y.; Yoon, Y. A biosensor platform for metal detection based on enhanced green fluorescent protein. *Sensors.* **2019**, *19* (8), 1846.

(11) Yagi, K. Applications of whole-cell bacterial sensors in biotechnology and environmental science. *Appl. Microbiol. Biot.* **2007**, *73* (6), 1251−1258.

(12) Moraskie, M.; Roshid, M. H. O.; O'Connor, G.; Dikici, E.; Zingg, J. M.; Deo, S.; Daunert, S. Microbial whole-cell biosensors: Current applications, challenges, and future perspectives. *Biosens. Bioelectron.* **2021**, *191*, 113359.

(13) Nagata, T.; Muraoka, T.; Kiyono, M.; Pan-Hou, H. Development of a luminescence-based biosensor for detection of methylmercury. *J. Toxicol. Sci.* **2010**, *35* (2), 231−234.

(14) Cui, Z. S.; Luan, X.; Jiang, H. C.; Li, Q.; Xu, G. F.; Sun, C. J.; Zheng, L.; Song, Y. Z.; Davison, P. A.; Huang, W. E. Application of a bacterial whole cell biosensor for the rapid detection of cytotoxicity in heavy metal contaminated seawater. *Chemosphere.* **2018**, *200*, 322−329.

(15) Peterson, L. A. Formation, repair, and genotoxic properties of bulky DNA adducts formed from tobacco-specific nitrosamines. *J. Nucleic. Acids.* **2010**, *2010*, 284935.

(16) Piepenbrock, M.-O. M.; Lloyd, G. O.; Clarke, N.; Steed, J. W. Metal- and anion-binding supramolecular gels. *Chem. Rev.* **2010**, *110* (4), 1960−2004.

(17) Zhang, J.; Su, C.-Y. Metal-organic gels: From discrete metallogelators to coordination polymers. *Coordin. Chem. Rev.* **2013**, *257* (7), 1373−1408.

(18) Wu, H.; Zheng, J.; Kjøniksen, A.-L.; Wang, W.; Zhang, Y.; Ma, J. Metallogels: availability, applicability, and advanceability. *Adv. Mater.* **2019**, *31* (12), 1806204.

(19) He, L.; Jiang, Z. W.; Li, W.; Li, C. M.; Huang, C. Z.; Li, Y. F. In situ synthesis of gold nanoparticles/metal-organic gels hybrids with excellent peroxidase-like activity for sensitive chemiluminescence detection of organophosphorus pesticides. *ACS. Appl. Mater. Inter.* **2018**, *10* (34), 28868−28876.

(20) Liang, H.; Jiang, S. H.; Yuan, Q. P.; Li, G. F.; Wang, F.; Zhang, Z. J.; Liu, J. W. Co-immobilization of multiple enzymes by metal coordinated nucleotide hydrogel nanofibers: improved stability and an enzyme cascade for glucose detection. *Nanoscale.* **2016**, *8* (11), 6071−6078.

(21) Sun, X. J.; Zhang, X.; Dong, H.; Yang, D. D.; Tang, H. L.; Zhai, Y. C.; Wei, J. Z.; Zhang, F. M. Porous metal-organic gel assisted by *L*-tartaric acid ligand for efficient and controllable drug delivery. *New J. Chem.* **2018**, *42* (18), 14789−14795.

(22) Zynel, C. A.; Wunder, B. A. Limits to food intake by the Prairie Vole: effects of time for digestion. *Funct. Ecol.* **2002**, *16* (1), 58−66.

(23) Lichtenberg-Frate, H.; Schmitt, M.; Gellert, G.; Ludwig, J. A yeast-based method for the detection of cyto and genotoxicity. *Toxicol in Vitro.* **2003**, *17* (5−6), 709−716.

(24) Lan, J. Q.; Rahman, S. M.; Gou, N.; Jiang, T.; Plewa, M. J.; Alshawabkeh, A.; Gu, A. Z. Genotoxicity assessment of drinking water disinfection byproducts by DNA damage and repair pathway profiling analysis. *Environ. Sci. Technol.* **2018**, *52* (11), 6565−6575.

(25) Lan, J. Q.; Gou, N.; Gao, C.; He, M.; Gu, A. Z. Comparative and mechanistic genotoxicity assessment of nanomaterials via a quantitative toxicogenomics approach across multiple species. *Environ. Sci. Technol.* **2014**, *48* (21), 12937−12945.

(26) Lan, J. Q.; Hu, M.; Gao, C.; Alshawabkeh, A.; Gu, A. Z. Toxicity Assessment of 4-methyl-1-cyclohexanemethanol and its metabolites in response to a recent chemical spill in west virginia, USA. *Environ. Sci. Technol.* **2015**, *49* (10), 6284−6293.

(27) Villar, M. L.; Godwin, I. R.; Hegarty, R. S.; Erler, D. V.; Farid, H. T.; Nolan, J. V. Nitrate and nitrite absorption, recycling and retention in tissues of sheep. *Small Ruminant. Res.* **2021**, *200*, 106392.

https://doi.org/10.1021/acs.nanolett.2c03418
Nano Lett. XXXX, XXX, XXX−XXX